

# Enhanced graphite passivation in Li-ion battery electrolytes containing disiloxane-type additive/co-solvent

Mariusz Walkowiak · Daniel Waszak ·  
Grzegorz Schroeder · Błażej Gierczyk

Received: 28 August 2008 / Revised: 7 October 2008 / Accepted: 13 October 2008 / Published online: 29 October 2008  
© Springer-Verlag 2008

**Abstract** This article reports the synthesis details and film-forming properties of 1,1,3,3-tetramethyl-1,3-bis(3-( $\omega$ -hexadecyloxy-deca(ethylenoxy)propyl)disiloxane, a new potential electrolyte additive/functional co-solvent for propylene carbonate (PC)-based Li-ion cells with graphitic anodes. Galvanostatic charge/discharge characteristics and scanning electron microscopy images provide direct evidence for the suppression of solvent intercalation and graphite exfoliation in the presence of the additive. In terms of irreversible capacity, the additive's efficiency is the highest for 15% weight ratio in the solvent mixture. Potentiodynamic measurements have revealed that disiloxane component undergoes irreversible reduction at potential significantly higher than PC decomposition. Energy dispersive spectroscopy analysis of graphite flake surfaces confirm that silicon species from the disiloxane decomposition are built in the passive layer. The reported compound may be considered as a basis for alternative cost-effective electrolyte compositions for low-temperature applications.

**Keywords** Li-ion battery electrolyte additives · Disiloxanes · Polyethers · Propylene carbonate · Graphite exfoliation · Solid electrolyte interphase

---

M. Walkowiak (✉) · D. Waszak  
Institute of Non-Ferrous Metals Branch in Poznań Central  
Laboratory of Batteries and Cells,  
Forteczna 12,  
61-362 Poznań, Poland  
e-mail: walkowiak@claiio.poznan.pl

G. Schroeder · B. Gierczyk  
Faculty of Chemistry, Adam Mickiewicz University,  
Grunwaldzka 6,  
60-780 Poznań, Poland

## Introduction

During first charging of a Li-ion cell, electrolyte components undergo reductive decomposition in contact with graphite anode. Products of this process are deposited on the graphite flakes surfaces in the form of passive layer, also called solid electrolyte interphase (SEI). SEI is permeable for lithium cations, therefore, allows for  $\text{Li}^+$  trespassing the electrode/electrolyte boundary and intercalation in the crystal structure of graphite active anode material. At the same time, SEI is electron-insulating, thus making the system kinetically stable in organic electrolytes. The structure and composition of SEI are extremely important as far as efficient and long-term operation of a Li-ion cell is considered. Viable electrolyte must contain a co-solvent responsible for the formation of proper SEI. In today's technological solutions, this role is played by ethylene carbonate (EC), despite of its well-known weaknesses. If the main solvent does not possess film-forming properties, an appropriate film-forming additive is necessary. The issue of film-forming electrolyte additives for Li-ion batteries has been subject of numerous research works (see review work by Zhang [1] for detailed overview of this topic). A typical example of electrolyte solvent requiring the addition of suitable film-forming additive (or film-forming co-solvent) is propylene carbonate (PC). PC may potentially be a very promising solvent for Li-ion cells due to its low melting point and excellent lithium-solvating characteristics. Unfortunately, PC has been proved to be incompatible with graphitic anodes, which is due to the fact that, upon first reduction, PC molecules tend to co-intercalate into the crystal structure of graphitic material together with  $\text{Li}^+$  cations, followed by its decomposition with the evolution of gaseous products [2–4]. Internal pressure created as a

result of this causes graphite flakes to exfoliate and whole cell to fail. Solvent co-intercalation in PC-based electrolytes may be suppressed, roughly speaking, in two ways. One of them is pre-treatment of graphite by suitable surface coating [5–8]. Another strategy is to apply appropriate film-forming electrolyte additive. It is widely accepted that film-forming additives can prevent PC co-intercalation according to one of three main mechanisms [1]: (a) electro-polymerisation of the additive monomers with the formation of a polymeric barrier against PC molecules (so-called polymerisable additives), (b) reductive decomposition of the additive molecules with the creation of protective passive film (so-called reduction-type additives) and/or (c) specific reactions involving the additive molecules and leading to the SEI stabilisation (so-called reaction-type additives). A significant number of SEI-enhancing electrolyte additives for PC-based electrolytes have been reported so far in the literature. Most of them have been described in [1]. Among the very recently reported molecular structures with proven ability of assisting the passive layer formation are, among others, silanes and siloxanes [9–13], isocyanates [14–17], methyl acetate [18], butyl sultone [19] and butylene sulphite [20].

In the present contribution, the film-forming properties of 1,1,3,3-tetramethyl-1,3-bis(3-( $\omega$ -hexadecyloxy-deca(ethylenoxy)propyl)disiloxane (for simplicity, designated hereinafter as DS10-16) have been reported. Polyether-functionalised siloxanes are easy to synthesise and, due to the presence of free electron pairs at ether oxygen atoms, have themselves excellent lithium-solvating properties, therefore, their addition does not affect inversely the electrolytes' conductivities.

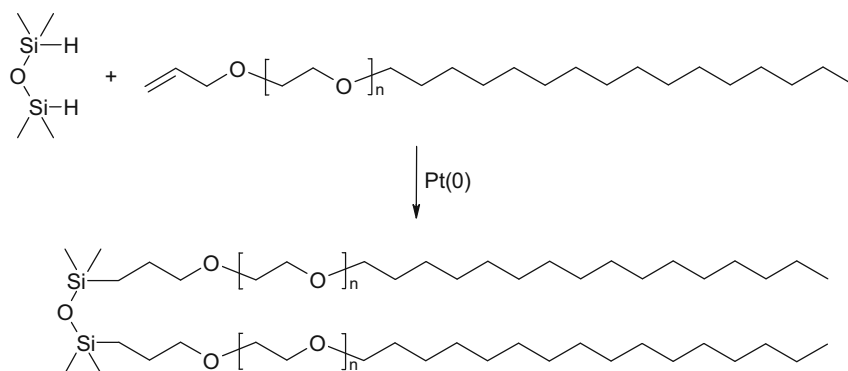
## Experimental

1,1,3,3-tetramethyl-1,3-bis(3-( $\omega$ -hexadecyloxy-deca(ethylenoxy)propyl)disiloxane has been synthesised according to Scheme 1).

Decaethylene glycol allyl hexadecyl ether was prepared from corresponding poly(oxaethylene glycol) hexadecyl ether (Brij 56;  $n \sim 10$ ) and allyl bromide by standard Williamson method [21]. The product was used for the next step without purification. To the 0.005-M solution of 1,1,3,3-tetramethyldisiloxane in anhydrous benzene, 0.01 mol of decaethylene glycol allyl hexadecyl ether and Karstedt catalyst (1,1,3,3-tetramethyl-1,3-divinylsiloxane-Pt(0) complex; 0.2 mol% per 1 mol of SiH bond) were added. The mixture obtained was stirred vigorously and refluxed under inert atmosphere until reaction was completed (checked by  $^1\text{H}$  NMR; about 10 h). After that the solvent was evaporated and a residual oil was filtered by a pad of Celite to remove the contaminating traces of Pt. The obtained product (acronym DS10-16) tends to solidify, forming a yellowish wax. Yield 95%, purity 98% ( $^1\text{H}$  NMR).  $^1\text{H}$  NMR ( $\text{CDCl}_3$ ):  $\delta$  -0.03 (s, 6H); 0.45 (t, 2H); 0.88 (t, 3H); 1.2–1.4 (m, 26H); 1.48 (q, 2H); 1.58 (q, 2H); 3.45 (t, 2H); 3.5–3.7 (m, 42H).  $^{29}\text{Si}$  NMR ( $\text{CDCl}_3$ ):  $\delta$  -58.8.

Electrolytes have been prepared by dissolving  $\text{LiPF}_6$  (Aldrich, 99.99%) in a mixture of PC (Merck, 99.7%, anhydrous) and DS10-16. For examination of the electrolyte behaviour during cathodic reduction, highly crystalline SL-20 graphite (Superior Graphite) was used as anode active material. The electrodes were prepared in a conventional way [9]. The cells were cycled galvanostatically at 10 mA/g of active electrode mass in the potential range 0–2 V vs.  $\text{Li/Li}^+$ . The cyclic voltammetry (CV) experiment was performed in two-electrode cell with the application of PAR model 273A potentiostat/galvanostat. Scan rate of  $0.05 \text{ mV s}^{-1}$  was applied. Scanning electron microscopy (SEM) observations of the graphite morphology and energy dispersive spectroscopy (EDX) microanalysis of passive layers have been carried out on graphite anodes removed from electrochemical cells after galvanostatic cycling with the application of Vega 5135MM apparatus, Tescan. The electrodes have been rinsed with propylene carbonate and dried under vacuum at  $120^\circ\text{C}$  for 24 h prior to investigations, so as to remove the remaining liquid electrolyte species. Anodic

**Scheme 1** 1,1,3,3-Tetramethyl-1,3-bis(3-( $\omega$ -hexadecyloxy-deca(ethylenoxy)propyl)disiloxane



stability of the electrolytes has been tested by means of linear sweep voltammetry (scan rate  $10 \text{ mV s}^{-1}$ , from the rest potential up to  $6 \text{ V vs. Li/Li}^+$ ) in two-electrode cells with lithium counter electrodes and platinum working electrodes (electrode area  $1 \text{ cm}^2$ ).

## Results and discussion

DS10-16 can be regarded as a member of a large family of podand-type compounds, i.e. compounds having, in their molecular structures, certain number of polyoxaethylene chains attached to a central atom or group of atoms. The examined compound has been designed and synthesised according to several prerequisites. First, strong solvating properties towards lithium salt have been ensured, so as to contribute to the overall conductivity of the solvent mixture. Electron donor properties, resulting from the existence of free electron pairs at ether oxygen atoms, give the DS10-16 molecule strong lithium cation-solvating ability. More than that, the flexibility of Si–O–Si bonds and special arrangement of the side chains is supposed to lead to self-organisation of the molecules in the presence of Li cations. This particular feature, characteristic for podand compounds, is likely to shield the “trapped” cation from the environment, thus further enhancing salt dissociation. Finally, aliphatic segments ending the polyether chains are known to further stabilise the complex with  $\text{Li}^+$ . Most importantly, later on in this paper, the property of suppressing PC co-intercalation into graphite will be unequivocally demonstrated. Component of this type can be described as “functional co-solvent”, by analogy to the concept of “functional electrolytes” first introduced by Abe et al. [22–23].

Figure 1 shows how constant current charge/discharge curves evolve as a function of the weight ratio of DS10-16 in the solvent mixture. For pure PC, the curve exhibits long plateau between  $0.8$  and  $1.0 \text{ V}$ , which is a common pattern for graphite anodes reduced in PC. The plateau is known to be connected with continuous excessive solvent reduction on multiple-split graphite surfaces formed during exfoliation. No reversible  $\text{Li}^+$  intercalation is observed. For  $5\% \text{ w/w}$  of DS10-16 in the solvent mixture, reversible capacity occurs with specific capacity of  $255 \text{ mAh g}^{-1}$  (see Table 1). The irreversible capacity is still very large ( $997 \text{ mAh g}^{-1}$ ), suggesting important degree of graphite exfoliation. For  $10\% \text{ w/w}$  of DS10-16, further decrease of the irreversible capacity can be seen ( $402 \text{ mAh g}^{-1}$ ) together with the increase of reversible capacity to  $289 \text{ mAh g}^{-1}$ . The  $15\% \text{ w/w}$  addition of DS10-16 results in charge/discharge characteristics resembling (in terms of general shape) the pattern known for standard Li-ion battery electrolytes. Part of the charge curve responsible for SEI formation does not reveal any traces of

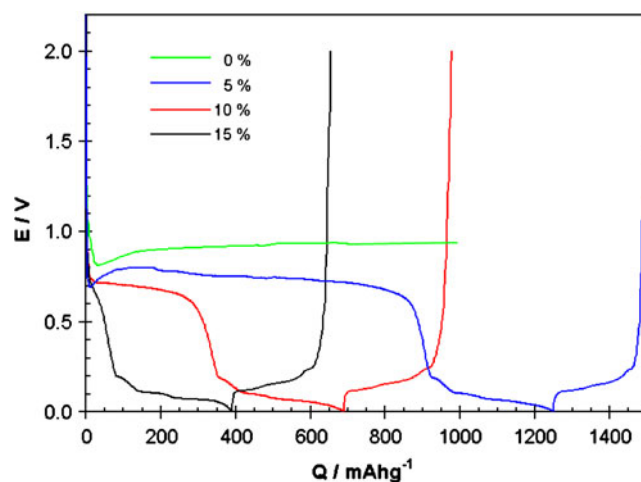


**Fig. 1** Galvanostatic charge/discharge characteristics in the first cycles recorded for graphite in PC-based electrolytes with various weight ratios of DS10-16

exfoliation behaviour. Certain drop of reversible capacity must be attributed to the increase of electrolyte viscosity caused by the addition of disiloxane.

SEM images taken from electrodes removed from the cells after charge/discharge tests (Fig. 2) allow for direct observation of graphite exfoliation phenomena. Typical exfoliated flake of graphite cycled in PC as sole solvent is shown in the Fig. 2a. Exfoliation-type morphology is still evident in the case of  $5\%$  and  $10\%$  of DS10-16 in the solvent mixture. At  $15\%$  of disiloxane, there are no visible traces of graphite exfoliation which directly proves that addition of the examined disiloxane suppresses PC co-intercalation. The effect seems to depend strongly on the additive weight percentage in the solvent mixture.

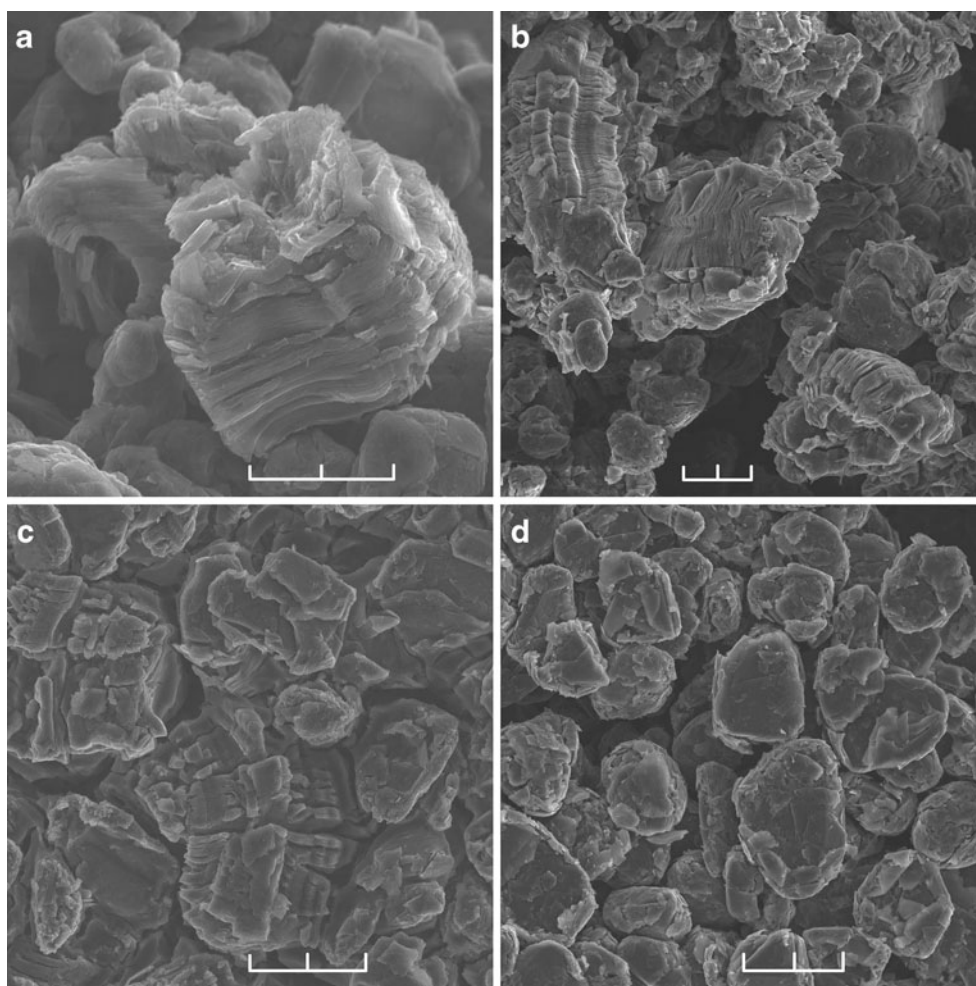
Cyclic voltammetry with slow scan rate (Fig. 3) has been performed for the electrolyte with  $15\% \text{ w/w}$  of DS10-16 in order to get insight into the mechanism of the suppression of solvent co-intercalation. On the first cycle loop, two irreversible current peaks can be clearly seen. The peak with maximum at approximately  $0.6 \text{ V}$  is typical for carbonaceous materials reduced in organic electrolytes and

**Table 1** Basic electrochemical parameters of graphite anodes galvanostatically charged/discharged in PC-based electrolytes with DS10-16

Solvent	$Q_{\text{rev}}$ ( $\text{mAh g}^{-1}$ )	$Q_{\text{irr}}$ ( $\text{mAh g}^{-1}$ )	Eff (%)	Exfoliation phenomena
PC	0	“∞”	0	Total exfoliation
PC/DS10-16 (5%)	255	997	20	Partial exfoliation
PC/DS10-16 (10%)	289	402	42	Partial exfoliation
PC/DS10-16 (15%)	263	129	67	No visible exfoliation

$Q_{\text{rev}}$  reversible capacity,  $Q_{\text{irr}}$  irreversible capacity,  $Eff$  Coulombic efficiency (in percentage terms) of charging in the first cycle

**Fig. 2** SEM images of graphite anodes removed from the cells after galvanostatic cycling in PC-based electrolytes with different weight ratios of DS10-16: **a** 0%, **b** 5%, **c** 10%, **d** 15%; white scales correspond to 20  $\mu\text{m}$



can be associated with the SEI formation as a result of PC and LIPF<sub>6</sub> decomposition. The peak with maximum at approximately 1.5 V is not that obvious and should most probably be attributed to the reductive decomposition of the disiloxane additive. The presence of this current signal indicates that the mechanism of beneficial action of disiloxane is connected to its reduction at high potentials, prior to the actual SEI formation. This type of mechanism has been widely discussed in the literature (compare review work [1]). Reduction-type additives typically undergo decomposition at relatively high potentials, providing a barrier preventing PC molecules from insertion into the crystal lattice of graphite.

So as to confirm the above conclusion, products of DS10-16 decomposition must be detected in the passive layers on graphite. EDX microanalysis provides the tool for detecting silicon species on the single flake surface. Figure 4 shows EDX spectrum measured over the area of a single graphite flake removed from the cell after cycling. As can be seen, spectrum of elements reveals important amounts of silicon and oxygen that inevitably come from the passive layer. Oxygen originates not only from disiloxane but also

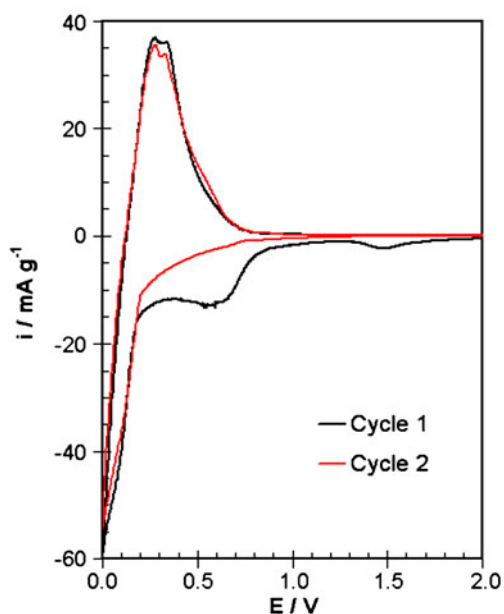


**Fig. 3** Cycling voltammetry curves in the first two cycles recorded for graphite in PC-based electrolyte with 15% w/w of DS10-16



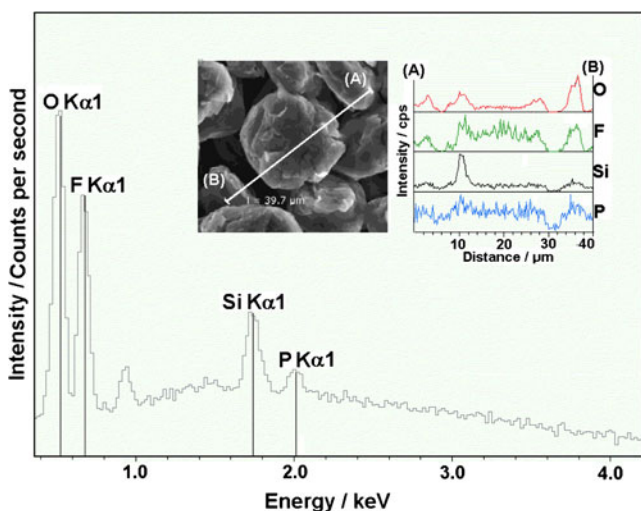


**Fig. 4** EDX microanalysis of passive layer on the graphite anode removed from the cell after galvanostatic charging/discharging in PC-based electrolyte with 15% w/w of DS10-16; in the *main frame*: spectrum of detected elements; in the *insets*: SEM image of the area of data acquisition and concentration profiles recorded for O, F, Si, and P

from PC decomposition. Phosphorus and fluorine signals, also present in the spectrum, obviously result from the decomposition products of  $\text{LiPF}_6$ . EDX spectrum thus evidences the reduction-type mechanism of the additive's suppressive properties towards graphite exfoliation. In the inset of Fig. 4, concentration profiles of four elements of interest are shown. The data have been collected along the white line shown in the SEM image. Signals from all the elements clearly prove their existence in measurable

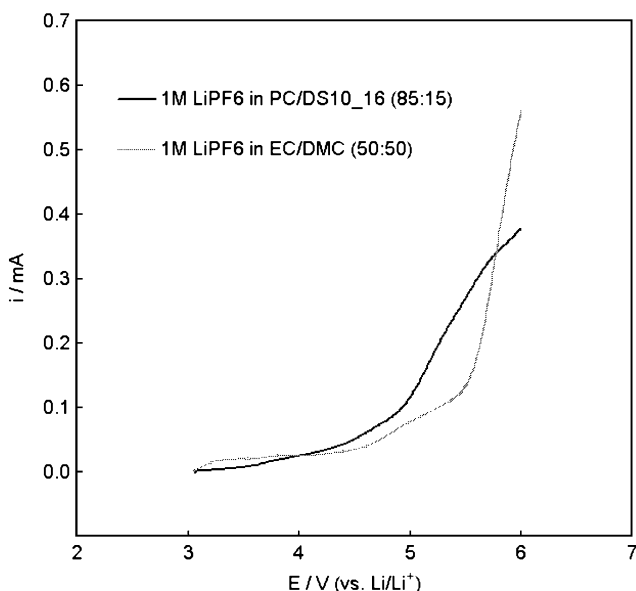


**Fig. 5** Linear sweep voltammetry curve recorded on Pt electrode for the electrolyte composition 1 M  $\text{LiPF}_6$  in PC/DS10-16 15%

amounts within the surface of flakes. Right beyond the flake edges, the corresponding signals abruptly drop.

Figure 5 presents the linear sweep voltammetry curve recorded on platinum electrode for the electrolyte with 15% w/w of DS10-16. For comparison, the analogous curve for a “standard” electrolyte composition (1 M  $\text{LiPF}_6$  in EC/DMC) has been shown. On the basis of the presented experiment, it is difficult to assess unequivocally the stability toward oxidation for the two examined electrolyte compositions. “Standard” electrolyte seems to start to decompose quickly at slightly higher potential. On the other hand, the PC-based electrolyte with DS10-16 additive features smaller decomposition current at 6 V. The real width of the electrochemical stability window should be ultimately determined in practical Li-ion cell. Further experiments, aiming at assessment of the performance of the studied electrolyte in Li-ion cell configuration (such as cycling stability, low temperature and high-rate capability), will be published in one of the future works.

## Conclusions

New film-forming additive/functional co-solvent for PC-based electrolytes has been reported. The contribution continues the efforts to identify silicon-based functional electrolyte components for Li-ion battery electrolytes. Constant current charge/discharge tests along with SEM images provide evidence for the suppression of PC molecule co-intercalation and graphite exfoliation, the effect strongly depending on the weight percentage of the disiloxane in the solvent mixture. Cyclic voltammetry curve and EDX microanalysis of graphite surfaces allow for the ascertainment that disiloxane additive undergoes decomposition at relatively high potential and builds in the possible layer, thus the reported compound can be classified as reduction-type additive. The proposed electrolyte composition requires more extensive tests on the feasibility of potential application. In this paper, resistance against electrochemical oxidation on platinum has been assessed and compared to a standard electrolyte composition.

**Acknowledgements** The work has been done in the frameworks of MNT-ERA-Net project NANOLION. Financial support from the Ministry of Science and Higher Education of Poland (grant no. ERA-NET MNT/93/22006) is gratefully acknowledged. The work was presented during the 9th International Conference “Advanced Batteries and Accumulators” (A.B.A.-9), Brno, Czech Republic, June 29–July 3, 2008.

## References

- Zhang SS (2006) J Power Sources 162:1379 doi:10.1016/j.jpowsour.2006.07.074

2. Dey AN, Sullivan BP (1970) *J Electrochem Soc* 117:222 doi:[10.1149/1.2407470](https://doi.org/10.1149/1.2407470)
3. Wagner MR, Raimann P, Möller KC, Besenhard JO, Winter M (2004) *Electrochem Solid-State Lett* 7:A201 doi:[10.1149/1.1739312](https://doi.org/10.1149/1.1739312)
4. Buqa H, Würsig A, Vetter J, Spahr ME, Krumeich F, Novak P (2006) *J Power Sources* 153:385 doi:[10.1016/j.jpowsour.2005.05.036](https://doi.org/10.1016/j.jpowsour.2005.05.036)
5. Gao J, Fu LJ, Zhang HP, Yang LC, Wu YP (2008) *Electrochim Acta* 53:2376 doi:[10.1016/j.electacta.2007.09.058](https://doi.org/10.1016/j.electacta.2007.09.058)
6. Fu LJ, Gao J, Zhang T, Cao Q, Yang LC, Wu YP, Holze R (2007) *J Power Sources* 171:904 doi:[10.1016/j.jpowsour.2007.05.099](https://doi.org/10.1016/j.jpowsour.2007.05.099)
7. Gao J, Zhang HP, Zhang T, Wu YP, Holze R (2007) *Solid State Ion* 178:1225 doi:[10.1016/j.ssi.2007.06.004](https://doi.org/10.1016/j.ssi.2007.06.004)
8. Gao J, Zhang HP, Fu LJ, Zhang T, Wu YP, Takamura T, Wu HQ, Holze R (2007) *Electrochim Acta* 52:5417 doi:[10.1016/j.electacta.2007.02.064](https://doi.org/10.1016/j.electacta.2007.02.064)
9. Schroeder G, Gierczyk B, Waszak D, Kopczyk M, Walkowiak M (2006) *Electrochem Commun* 8:523 doi:[10.1016/j.elecom.2006.01.021](https://doi.org/10.1016/j.elecom.2006.01.021)
10. Schroeder G, Gierczyk B, Waszak D, Walkowiak M (2006) *Electrochem Commun* 8:1583 doi:[10.1016/j.elecom.2006.07.030](https://doi.org/10.1016/j.elecom.2006.07.030)
11. Xia Q, Wang B, Wu YP, Luo HJ, van Ree T (2008) *J Power Sources* 180:602 doi:[10.1016/j.jpowsour.2008.01.039](https://doi.org/10.1016/j.jpowsour.2008.01.039)
12. Walkowiak M, Waszak D, Schroeder G, Gierczyk B (2008) *Electrochem Commun* doi:[10.1016/j.elecom.2008.08.036](https://doi.org/10.1016/j.elecom.2008.08.036)
13. Walkowiak M, Waszak D, Gierczyk B, Schroeder G (2008) *Cent Eur J Chem* doi:[10.2478/s11532-008-0058-8](https://doi.org/10.2478/s11532-008-0058-8)
14. Korepp C, Kern W, Lanzer EA, Raimann PR, Besenhard JO, Yang M, Möller K-C, Shieh D-T, Winter M (2007) *J Power Sources* 174:628 doi:[10.1016/j.jpowsour.2007.06.140](https://doi.org/10.1016/j.jpowsour.2007.06.140)
15. Korepp C, Kern W, Lanzer EA, Raimann PR, Besenhard JO, Yang M, Möller K-C, Shieh D-T, Winter M (2007) *J Power Sources* 174:387 doi:[10.1016/j.jpowsour.2007.06.141](https://doi.org/10.1016/j.jpowsour.2007.06.141)
16. Korepp C, Santner HJ, Fujii T, Ue M, Besenhard JO, Möller K-C, Winter M (2006) *J Power Sources* 158:578 doi:[10.1016/j.jpowsour.2005.09.021](https://doi.org/10.1016/j.jpowsour.2005.09.021)
17. Zhang SS (2006) *J Power Sources* 163:567 doi:[10.1016/j.jpowsour.2006.09.046](https://doi.org/10.1016/j.jpowsour.2006.09.046)
18. Kim W-S, Park D-W, Jung H-J, Choi Y-K (2006) *Bull Korean Chem Soc* 27:82
19. Xu MQ, Li WS, Zuo XX, Liu JS, Xu X (2007) *J Power Sources* 174:705 doi:[10.1016/j.jpowsour.2007.06.112](https://doi.org/10.1016/j.jpowsour.2007.06.112)
20. Chen R, Wu F, Li L, Gyan Y, Qiu X, Chen S, Li Y, Wu S (2007) *J Power Sources* 172:395 doi:[10.1016/j.jpowsour.2007.05.078](https://doi.org/10.1016/j.jpowsour.2007.05.078)
21. Williamson A (1850) *Philos Mag* 37:350
22. Abe K, Yoshitake H (2004) *Electrochemistry* 72:519
23. Abe K, Miyoshi K, Hattori T, Ushigoe Y, Yoshitake H (2008) *J Power Sources* 184:449 doi:[10.1016/j.jpowsour.2008.03.037](https://doi.org/10.1016/j.jpowsour.2008.03.037)